ResearchGate

See discussions, stats, and author profiles for this publication at: https://www.researchgate.net/publication/236018160

Spectroscopical analysis of luminescent silicon rich oxide films

Article *in* Revista Mexicana de Fisica · December 2007

CITATIONS
9

READS
50

7 authors, including:

Alfredo Morales
Centro de Investigación en Materiales Avanzad…
75 PUBLICATIONS 446 CITATIONS

SEE PROFILE

Carlos Domínguez
Spanish National Research Council
274 PUBLICATIONS 3,028 CITATIONS

SEE PROFILE

Mariano Aceves
Instituto Nacional de Astrofísica, Óptica y Elect…
176 PUBLICATIONS 753 CITATIONS

SEE PROFILE

J. A. Luna López
Benemérita Universidad Autónoma de Puebla
103 PUBLICATIONS 438 CITATIONS

SEE PROFILE

Some of the authors of this publication are also working on these related projects:

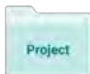

Study and development of Cu2ZnSnS4 thin-films obtained by sputtering for their possible aplication in fotovoltaic devices. View project

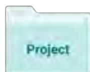

Studies and Integration of Silicon Based Light Emitting Systems View project

All content following this page was uploaded by Carlos Domínguez on 13 January 2014.

The user has requested enhancement of the downloaded file.

REVISTA MEXICANA DE FÍSICA S **53** (7) 279–282 DICIEMBRE 2007

Spectroscopical analysis of luminescent silicon rich oxide films

A. Morales*, C. Domínguez, J. Barreto, and M. Riera
IMB-CNM, CSIC, Campus UAB,
08193 Bellaterra, Barcelona, España,
e-mail: alfredo.morales@cnm.es

M. Aceves, J.A. Luna, Z. Yu, and R. Kiebach
INAOE,
Apartado postal 51, 72000 Puebla, Pue., México.

Recibido el 30 de noviembre de 2006; aceptado el 8 de octubre de 2007

Compositional, structural and optical properties of silicon rich oxide (SRO) films containing different silicon excess were investigated using X ray photoelectron spectroscopy (XPS), Raman spectroscopy, energy filtered transmission electron microscopy (EFTEM) and photoluminescence (PL). The XPS-Si2p peaks fitting showed the presence of $Si - Si_4$ tetrahedra only for the SRO film with the highest silicon excess. Raman spectroscopy revealed amorphous phase silicon in the SRO films with lowest silicon excess; when it was increased, a sharp peak at around 517 cm^{-1} appeared, which corresponds to crystalline silicon. Si-nanoclusters were slightly observed by EFTEM in the SRO film with the lowest silicon content. They became more evident when the silicon excess was increased, in agreement to Raman spectra. A strong PL was observed in the SRO films with low silicon excess. However, in SRO films with the highest silicon excess, where the silicon agglomeration is greater, the PL practically disappeared. According to these results, we have analysed the dependence of photoluminescence on the composition and structure of the SRO films.

Keywords: Silicon rich oxide; Silicon clusters; Raman; XPS; EFTEM; Photoluminescence.

La composición, estructura y propiedades ópticas de películas de óxido rico en silicio (SRO) con diferentes excesos de silicio fueron investigadas usando espectroscopía de fotoelectrones de rayos X (XPS), espectroscopía Raman, microscopía electrónica de transmisión con energía filtrada (EFTEM) y fotoluminiscencia (FL). El ajuste de los picos XPS-Si2p solo mostraron la presencia de tetrahedros $Si - Si_4$ en la película de SRO con más alto contenido de silicio. La espectroscopía Raman reveló una fase de silicio amorfo en películas de SRO con más bajo exceso de silicio, cuando este se incrementó, apareció un pico en 517 cm^{-1}, el cual corresponde a silicio cristalino. Mediante EFTEM, nano-aglomerados de silicio fueron ligeramente observados en las películas con el más bajo exceso de silicio. Estos llegaron a ser más evidentes cuando el exceso de silicio se incrementó, en acuerdo con los espectros Raman. Las películas de SRO con bajo exceso de silicio mostraron una fuerte FL. Sin embargo, para mayor exceso de silicio, donde la aglomeración es mayor, la FL prácticamente desapareció. La dependencia de la FL con respecto de la composición y estructura de las películas de SRO ha sido analizada.

Descriptores: Óxido rico en silicio; aglomerados de silicio; Raman; XPS; EFTEM; fotoluminiscencia.

PACS: 82.80.Gk; 79.60.-i; 68.37.Lp; 78.55.-m

1. Introduction

It is known that bulk silicon is not an appropriate material to exhibit light emission properties, due to its indirect band gap. Several silicon (Si) based materials have been reported to solve the physical inability of silicon to act as light emitter, including porous silicon [1, 2], hydrogenated silicon rich oxynitride [3], multilayers [4, 5] and silicon rich oxides (SiO_x, x<2) [6–9]. The key for the excellent light emission properties in these materials are the embedded silicon nanoparticles. Because porous silicon lacks chemical stability and robustness, Si-rich oxides seem to be a better alternative. A great variety of techniques to produce Si-nanoparticles have been reported, such as Si ion implantation into thermally grown SiO_2 films [10, 11], co-sputtering [7,12], Pulsed laser deposition [9,13], low pressure chemical vapor deposition (LPCVD) [14], plasma enhanced chemical vapor deposition (PECVD) [3, 5, 6, 15], etc. In this work, we present a study about phase separation in SRO films deposited on silicon substrates by LPCVD. An analysis of the Si2p peak obtained in XPS spectra was performed by taking the random bonding model (RBM) [14, 16] into account. Different silicon environments were obtained for each SRO film, depending on the silicon excess. Raman spectroscopy was used to observe the formation of a crystalline or amorphous silicon phase. EFTEM was used to confirm the level of silicon agglomeration, leading to the formation of silicon clusters (Si-clusters) inside the SRO films. These nanoparticles were more obvious in the SRO films with silicon excess greater than 5.1 at.%. The mean particle size increases with higher silicon excess. Contrary to this, a higher PL intensity for the SRO films with low silicon excess was observed. Therefore, the relation between structure and optical properties is analyzed.

2. Experiment

SRO films were deposited on n type (100) silicon substrates by LPCVD hot wall reactor at 700°C using N_2O and SiH_4 as

the reactant gasses. The flow ratio (Ro), N_2O/SiH_4, was used to control the amount of silicon excess in the films. The thickness of the films was around 700 nm. After deposition, SRO films were thermally annealed at 1100°C for 60 minutes in N_2 atmosphere. The thickness and the refractive index were measured with a Gaertner L117 ellipsometer. X-ray photoelectron spectroscopy (XPS) analysis was carried out using a PHI ESCA-5500 spectrometer with a monochromatic Al radiation and energy 1486 eV. Energy Filtered Transmission Electron Microscopy (EFTEM) images were obtained using an electronic microscopy JEOL JEM 2010F. Raman spectra were recorded using an Ar+ laser operating at a wavelength of 488 nm. PL at room temperature were carried out with a Perkin Elmer luminescence spectrometer; model LS50B, which is controlled by computer. The samples were excited using a 250 nm (4.96 eV) radiation. PL spectra were scanned in the 400-900 nm with a resolution of 2.5 nm .

3. Results

Table I summarizes the thickness and refractive index of the deposited SRO films measured by null ellipsometry. The variation of the refractive index as the flow ratio Ro changes shows the presence of excess silicon in the films. Results for the silicon excess of the different samples from XPS analyses are also presented in Table I; the value ranges from 4 to 12.7 at.%.

There are two models describing the microstructure of SiO_x ($x < 2$) films. First, the random bonding model (RBM) [14, 16], in which the silicon environment can be distinguished between five different tetrahedral units, Si-(Si_{4-n}-O_n) with n=0-4, corresponding to five possible oxidation states of silicon (Si°, Si^{1+}, Si^{2+}, Si^{3+} and Si^{4+}). The second model, the random mixtures model (RMM) [14, 17], suggests SiO_x ($x < 2$) films consist of $Si-Si_4$ (Si°) and Si-O_4 (Si^{4+}) tetrahedras, neglecting the existence of intermediate states.

Figure 1 presents the XPS Si2p peak of the $SRO_{12.7}$, $SRO_{5.1}$, SRO_4 films annealed at 1100°C; the sub-index in the notation refers to the silicon excess. According to the RMM model, the $SRO_{5.1}$ and SRO_4 films should be stoichiometric; however, a phase separation must take place in these samples by the high annealing temperature (≫700°C) and because a phase separation starts at temperatures of 400-700°C [6, 13]. The peak energy shifted toward lower energy when the silicon excess was increased, at the same time that the distribution width became broader, indicating the contribution of different oxidation states, in agreement with the description of the RBM model. The inset of figure 1 shows the fitting Si2p peak for SRO_4 film using Gaussian components. A contribution of two peaks placed at 101.9 and 104.4 eV related to Si^{2+} (Si-Si_2O_2) and Si^{4+} (Si-O_4), respectively, has been found. The biggest component is associated to pure silicon dioxide, as expected due to the low silicon excess. The fitting of the Si2p peak for $SRO_{5.1}$ film produced the same oxidation states, Si^{2+} and Si^{4+}, but an increase in the area of the Si^{2+} peak was observed, as shown in table II. The presence of Si° was not observed in any of these films indicating the absence of Si-Si_4 tetrahedra. The low silicon excess in these films could be the cause of this behaviour, that is, the phase separation forming Si-clusters inside of a SiO_2 matrix could be present; however, it is possible that the size of Si-clusters compared to the SiO_2 matrix surround them is relatively small, being easier to detect the Si-O_4 component in the Si2p peak. When the silicon excess was increased ($SRO_{12.7}$), the Si2p spectra displayed an asymmetrical peak, indicative of the presence of bigger concentration of suboxide components. In this film, the fitting produced, in addition to the Si^{2+} and Si^{4+} peaks, the peak corresponding to Si°, indicating the presence of elemental silicon. Nevertheless, the area corresponding to suboxides, Si° and Si^{2+}, was smaller than the SiO_2 (Si^{4+}) area. Table II shows the peaks and area from different oxidation states.

In Fig. 2, the Raman spectra from the SRO films after thermal annealing at 1100°C is shown. A peak at around

TABLE I. Characteristics of the SRO films.

Ro = N_2O/SiH_4	Thickness (nm)	Refractive index	Si excess (at.%)
10	770	1.99	12.7
20	730	1.64	5.1
30	720	1.48	4.0

TABLE II. Oxidation states obtained from the Si2p peaks.

Oxidation	$SRO_{12.7}$		$SRO_{5.1}$		SRO_4	
state	Peak	Area	Peak	Area	Peak	Area
Si^0	98.7	0.52	-	-	-	-
Si^{2+}	101.8	22.3	101.8	4.6	101.9	1.4
Si^{4+}	104.1	32.5	103.9	48.9	104.4	58.5

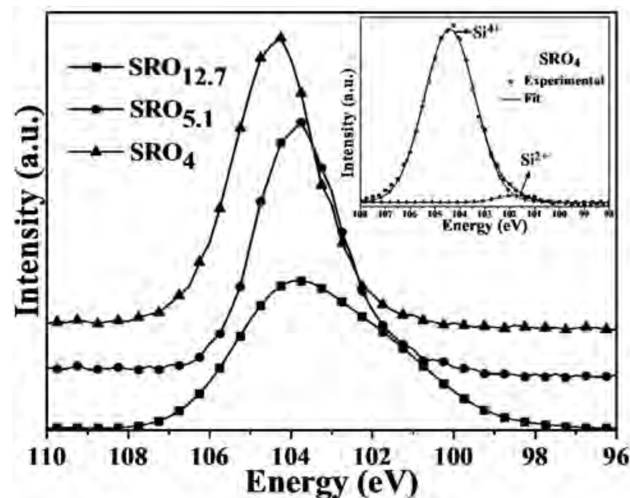

FIGURE 1. Variation of the Si2p peak in the SRO films thermally annealed at 1100°C with respect to the silicon excess. Inset: Si2p peak fitting of the SRO_4 film.

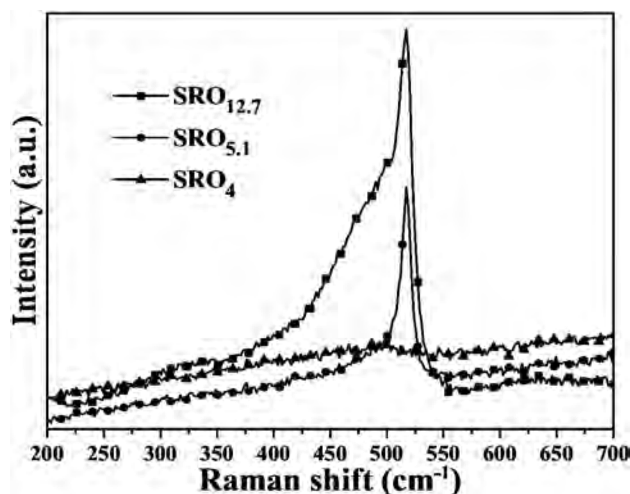

FIGURE 2. Raman spectra of the SRO films after thermal annealing at 1100°C.

517 cm^{-1} indicates the presence of crystalline silicon [8, 9, 13] in the SRO films with silicon excess ≥ 5.1 at.% ($SRO_{5.1}$ and $SRO_{12.7}$); its intensity decreases with lower silicon excess. In addition, a broad peak at 480 cm^{-1} is observed, which is due to an amorphous silicon phase [5, 9, 13], being most intense for the film with the highest silicon excess, the $SRO_{12.7}$ film. For the SRO film with the lowest silicon excess (SRO_4), a broad peak with low intensity in the area ranging from 430 to 530 cm^{-1} with a maximum at around 492 cm^{-1}, is observed, which was attributed to a-Si. The Raman results concerning phase separation (between Si and SiO_2) in the $SRO_{12.7}$ film agree with the Si2p fitting analysis.

In order to corroborate Si-clusters formed inside of the SRO films after thermal annealing, the samples were analyzed by means of the EFTEM technique. Figure 3 shows the EFTEM images for the SRO films thermally annealed at 1100°C for 60 minutes. The bright zones are associated to silicon nanoparticles in the film. The EFTEM image for the SRO_4 film shown in Fig. 3 a indicates some slightly bright zones. Because of low contrast and sharpness, the contour of the Si particles is not clear. Taking into consideration the results discussed above for SRO_4 from Raman spectroscopy, the silicon clusters observed in this film are expected to be amorphous. As expected, a phase separation between Si and SiO_2 becomes more evident when the silicon excess increases. Figure 3b) shows the EFTEM image for the $SRO_{5.1}$ film, where more well-defined Si-nanoclusters were observed. The size of the Si-clusters is in the 1.5 to 4 nm range, with an average size of 2.7 nm. The largest Si-clusters were observed in the SRO film with the highest silicon excess (Fig. 3c). While some show an elliptical shape, others have an enlarged one, which could be a result of the agglomeration of neighboured Si-clusters. A great dispersion of sizes is observed; the size is in the 0.5 to 7.5 nm range, the mean size being around 4.1 nm. Therefore, the phase separation observed by Raman is confirmed with the EFTEM results.

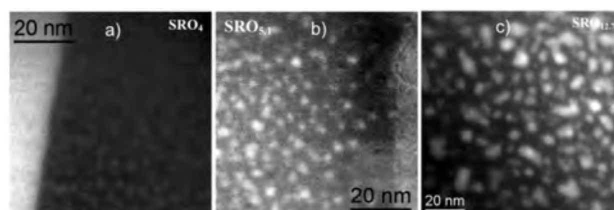

FIGURE 3. EFTEM images from the SRO films with a) 4 at.%, b) 5.1 at.% and c) 12.7 at.% of silicon excess and annealed at 1100°C for 60 minutes.

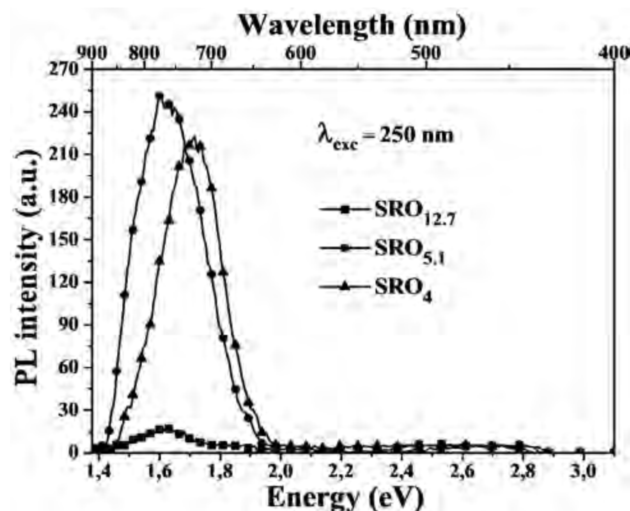

FIGURE 4. PL spectra from SRO films annealed at 1 100°C for 60 minutes.

Figure 4 shows the PL spectra of the SRO films thermally annealed. All films exhibited a PL band in the red region from the visible spectra. A dependence of the energy and intensity of the photoluminescence peak on the silicon excess is recognizable. For SRO_4, a PL peak at about 1.69 eV appears with a high intensity, even observable with the naked eye. A red-shift (towards 1.62 eV) and an increase in the intensity were observed for a silicon excess of 5.1 at.% ($SRO_{5.1}$). However, the sample with the highest silicon excess ($SRO_{12.7}$) emits at the same peak position (1.62 eV) regardless of difference in the mean size of the Si clusters, 4.1 nm for $SRO_{12.7}$ and 2.7 nm for $SRO_{5.1}$. Besides, the intensity was reduced by a factor of almost 20 times for $SRO_{12.7}$.

4. Discussion

It is widely accepted that Si-clusters are created when the SRO films are subjected to high temperature anneal because the thermal annealing produces a phase separation between Si and SiO_2. Although the fitting of the XPS Si2p peak of the SRO_4 and $SRO_{5.1}$ did not show the presence of a silicon phase, the Raman spectra does. The results indicated that a complete phase separation took place. EFTEM images corroborated the presence of Si-clusters inside of the SRO films, where their mean size and density increased as the silicon

excess was greater, according to other results [6–8]. The Si-clusters inside of the SRO_4 film were slightly observed; apparently, with a smaller mean size than the one observed in the $SRO_{5.1}$.

The mechanism of light emission observed in silicon-based materials where Si-nanoparticles are embedded has not yet been completely understood. Some defects have been shown to act as radiative recombination centers [10, 11]. So, luminescence in the blue region of the visible spectra has been related to defects such as neutral oxygen vacancies [11]. However, the emission in longer wavelengths has been explained according to two models: the first one describes that the luminescence take place in silicon nanocrystals (Si-nc's) by quantum confinement effects (QCE) [3, 6, 9, 15]. The second model relates the PL with the presence of defects in the SiO_2/Si-nc matrix and/or interface [1, 2, 4, 7, 8, 10, 11]. The PL band in 1.62 eV could be correlated to the Si-nanoclusters inside of the $SRO_{5.1}$ film; however, in the $SRO_{12.7}$ film (highest silicon excess) where the size of the Si-clusters increased, the PL band strongly reduced and no redshift was observed, contrary to the QCE model. Therefore, we think that another mechanism is responsible for the emission in these SRO films. A possible explanation is the presence of defects at the interface Si-cluster/SiO_2. In fact, it has been reported that a SiO_x shell exists at the surface of the Si-clusters and then a SiO_2 matrix [5, 12]. In the SiO_x matrix, some defects could exist. Then, we can consider that the Si clusters are surrounded by defects and they could be acting as localized states. Therefore, e-h pairs could be generated inside of the Si-clusters and the emission taking place between the localized state and the ground state. When the size of the Si-Clusters is bigger, the band gap energy decreases, and then the separation between the localized state and the ground state is also reduced. As their size increases even more, this separation is even more reduced, and eventually, when the size exceeds an optimum size, the energy of the localized state will be localized out of the Si-cluster band-edge, and then PL will not be observed, as occurs in the $SRO_{12.7}$ film. A maximum PL intensity was observed in the SRO films where the mean size of Si-clusters is around 2.7 nm, so we could consider it as the optimum size for these experiments.

5. Conclusions

We have studied the composition, structure and optical properties of SRO films obtained by LPCVD annealed at 1100°C and with different silicon excess. The phase separation was analyzed using the XPS Si2p peaks and Raman spectroscopy. From the Si2p peak, we deduce that a phase separation took place in the SRO films with the highest silicon excess. The phase separation observed by Raman spectroscopy was corroborated by EFTEM images. EFTEM analysis showed Si-nanoclusters in the SRO films, being more evident with silicon excess higher than 5.1 at.%. The average size of the Si-clusters varied according to the silicon excess. A strong PL was obtained in SRO films with 4 and 5.1 at.% of silicon excess annealed at 1100°C. A redshift only took place when the silicon excess was increased between these two films. The photoluminescence strongly reduced when the Si-clusters size was 4.1 nm ($SRO_{12.7}$). Then, the PL origin was ascribed to defects surrounding the Si-clusters. The biggest PL intensity was obtained with the SRO films containing 5.1 at.% of silicon excess annealed at 1100°C, which contains Si-clusters of 2.7 nm in mean size.

Acknowledgments

A. Morales and J. Barreto acknowledges the grants received from CONACYT-FC and I3P CSIC, respectively. This work has been partially supported by the project NANOMAGO: MAT2002-04484, financed by the Spanish Ministry of Education and Science, and by CONACYT and FOMIX Puebla.

1. J.Q. Duan *et al.*, *J. Appl. Phys.* **78** (1995) 478.
2. G.G. Qin and Y.Q. Jia, *Solid state Communications* **86** (1993) 559.
3. S. Kohli *et al.*, *Nanotechnology* **15** (2004) 1831.
4. L. Khriachtchev, S. Novikov, and J. Lahtinen, *J. Appl. Phys.* **92** (2002) 5856.
5. X.L. Wu *et al.*, *Appl. Phys. Lett.* **69** (1996) 523.
6. X.Y. Chen *et al.*, *J. Appl. Phys.* **97** (2005) 014913-1.
7. Y. Zankawa, S. Hayashi, and K. Yamamoto, *J. Phys.: Condens. Matter* **8** (1996) 4823.
8. T. Inokuma *et al.*, *J. Appl. Phys.* **83** (1998) 2228.
9. X.Y. Chen *et al.*, *J. Appl. Phys.* **96** (2004) 3180.
10. H.Z. Song and X. M Bao, *Phys. Rev. B* **55** (1997) 6988.
11. H.Z. Song, X.M. Bao, N.S. Li, and J.Y. Zhang, *J. Appl. Phys.* **82** (1997) 4028.
12. P.T. Huy, V.V. Thu, N.D. Chien, C.A.J. Ammerlaan, and J. Weber, *Physica B* **376-377** (2006) 868.
13. E. Fazio, E. barletta, F. Barreca, F. Neri, and S. Trusso, *J. Vac. Sci. Technol. B* **23** (2005) 519.
14. F. Iacona, S. Lombardo, and S.U. Campisano, *J. Vac. Sci. Technol. B* **14** (1996) 2693.
15. S. Tong, X. Liu, T. Gao, and X. Bao, *Appl. Phys. Lett.* **71** (1997) 698.
16. H.R. Philipp, *J. of Non-crystalline Solids* **8-10** (1972) 627.
17. R.J. Temkin, *J. of Non-crystalline Solids* **17** (1975) 215.